



## A concise account of techniques available for shipboard sea state estimation

Nielsen, Ulrik Dam

*Published in:*  
Ocean Engineering

*Link to article, DOI:*  
[10.1016/j.oceaneng.2016.11.035](https://doi.org/10.1016/j.oceaneng.2016.11.035)

*Publication date:*  
2017

*Document Version*  
Peer reviewed version

[Link back to DTU Orbit](#)

*Citation (APA):*  
Nielsen, U. D. (2017). A concise account of techniques available for shipboard sea state estimation. *Ocean Engineering*, 129, 352-362. <https://doi.org/10.1016/j.oceaneng.2016.11.035>

---

### General rights

Copyright and moral rights for the publications made accessible in the public portal are retained by the authors and/or other copyright owners and it is a condition of accessing publications that users recognise and abide by the legal requirements associated with these rights.

- Users may download and print one copy of any publication from the public portal for the purpose of private study or research.
- You may not further distribute the material or use it for any profit-making activity or commercial gain
- You may freely distribute the URL identifying the publication in the public portal

If you believe that this document breaches copyright please contact us providing details, and we will remove access to the work immediately and investigate your claim.

# A Concise Account of Techniques Available for Shipboard Sea State Estimation

Ulrik Dam Nielsen<sup>1,2\*</sup>

<sup>1</sup>*DTU Mechanical Engineering, Technical University of Denmark, DK-2800 Kgs. Lyngby, Denmark*

<sup>2</sup>*Centre for Autonomous Marine Operations and Systems, AMOS-NTNU, NO-7491 Trondheim, Norway*

**ABSTRACT.** This article gives a review of techniques applied to make sea state estimation on the basis of measured responses on a ship. The general concept of the procedures is similar to that of a classical wave buoy, which exploits a linear assumption between waves and the associated motions. In the frequency domain, this assumption yields the mathematical relation between the measured motion spectra and the directional wave spectrum. The analogy between a buoy and a ship is clear, and the author has worked on this *wave buoy analogy* for about fifteen years. In the article, available techniques for shipboard sea state estimation are addressed, but with a focus on only the wave buoy analogy. Most of the existing work is based on methods established in the frequency domain but, to counteract disadvantages of the frequency-domain procedures, newer studies are working also on procedures formulated directly in the time domain. Sample results from several studies are included, and the main findings from these are mentioned.

**Key words:** Sea state estimation; Wave buoy analogy; Vessel responses; Frequency domain; Time domain.

## 1. INTRODUCTION

In today's maritime world, the operation of ships requires careful monitoring of the related costs while, at the same time, ensuring a high level of safety. Shipboard decision support systems may enable a ship's crew to reduce costs and minimise risks while sailing, so that the performance is optimised. A ship's performance with respect to safety and fuel efficiency is in general negatively influenced by the encountered waves. Consequently, it is of particular importance to estimate the surrounding sea state, and any shipboard decision support system needs to have information about the encountered waves as input for the system to be the most accurate and reliable.

---

\*Email: udn@mek.dtu.dk

16 Trustful means for sea state estimation include floating wave buoys, which are primary tools used to collect  
17 statistical ocean wave data. However, wave buoys are not practical for a sailing ship requiring (precise) sea  
18 state information in real-time and at its actual geographical position. On the other hand, the analogy between  
19 a ship and a floating buoy naturally suggests to using the ship itself as a kind of wave buoy. Thus, a number  
20 of research studies have explored this 'wave buoy analogy' in the past, and the author of the present paper  
21 has worked extensively on the topic for about the last fifteen years.

22 This paper presents a concise account of techniques for shipboard sea state estimation using measured vessel  
23 responses, resembling the concept of a traditional wave buoy. Moreover, newly developed ideas for ship-  
24 board sea state estimation are introduced. The account, or review, is not necessarily complete, as it primarily  
25 reflects the author's personal experience and background; obtained alone and together with national as well  
26 as international colleagues. However, it is believed that the author has come across most of the work carried  
27 out within the particular field, so other fundamental studies, not related to the present author, will also be  
28 cited; without the ambition to list every single reference from the literature.

29 Although other means for shipboard sea state estimation exist, based on, e.g., the use of X-band navigational  
30 radars or over-the-bow looking devices, those means will not be mentioned herein and, hence, shipboard  
31 sea state estimation refers in the following to only the wave buoy analogy, where sea state estimation is  
32 conducted on the basis of measured vessel responses. Onwards, *sea state estimation* will at most places be  
33 shortened by SSE.

34 **1.1. Past Work and Literature.** Until the 1970'ies, little work on shipboard SSE had been done, but early  
35 researches (e.g. Lindemann and Nordenstrøm, 1975; Lindemann et al., 1977; Robinson, 1990; Debord and  
36 Hennessy, 1990; Francescutto, 1993) on in-service monitoring systems combined with decision support  
37 tools emphasised the need for estimates of the on-site sea state; at the actual position of the advancing  
38 vessel. Some of the initial studies on shipboard SSE (Takekuma and Takahashi, 1973; Pinkster, 1978) did  
39 not consider ships with forward speed, and although attempts were made to introduce forward speed in  
40 shipboard SSE, notably by Japanese studies (Isobe et al., 1984; Kobune and Hashimoto, 1986; Hirayama,  
41 1987; Iseki et al., 1992; Saito et al., 2000; Maeda et al., 2001), the first study to strictly consider the Doppler  
42 shift, implying a 1-to-3 relationship between encounter frequency and wave frequency for certain conditions  
43 in following sea, was made by Iseki and Ohtsu (2000). Since then several studies with good results have  
44 been published for ships with forward speed (Iseki and Terada, 2002; Iseki, 2004; Nielsen, 2006; Nielsen  
45 and Stredulinsky, 2012; Nielsen and Iseki, 2012; Nielsen et al., 2013; Montazeri et al., 2016a; Montazeri,  
46 2016); all considering full-scale data of different vessels. A number of studies have also been made in  
47 relation to station keeping and dynamic positioning, where shipboard SSE has been made with success for

48 ships without forward speed (Waals et al., 2002; Tannuri et al., 2003; Pascoal et al., 2007; Simos et al., 2007;  
49 Sparano et al., 2008; Pascoal and Soares, 2009).

50 **1.2. Content and Composition of Paper.** Different mathematical models exist for the wave buoy analogy,  
51 and the main principles will be outlined in Section 2. It is shown that shipboard SSE can be carried out either  
52 in the frequency domain or in the time domain, and, based on the setting, Sections 3 and 4 provide summaries  
53 of the fundamental assumptions and the different mathematical models which are applied depending on the  
54 particular domain, being it time or frequency. Sample results taken from several of the author's previous  
55 application studies, relating to both frequency and time domain calculations, are included in Section 5.  
56 Finally, concluding remarks are given in Section 6.

## 57 2. WAVE BUOY ANALOGY

58 Most of today's marine vessels are instrumented with sensors to record, e.g., global motion components such  
59 as heave, pitch, and vertical acceleration at specific position(s) relative to the centre of gravity. In this sense,  
60 vessels resemble classical wave buoys; although the latter typically have much simpler geometrical forms  
61 compared to the hull of a ship. Anyhow, the response recordings from marine vessels can be processed  
62 to facilitate estimation of the on-site sea state, making the analogy to floating wave buoys by relating the  
63 measurements and the sea state through a mathematical model, see Figure 1.

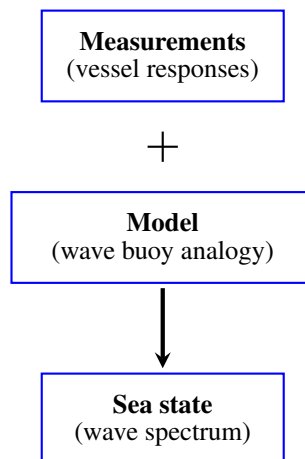


FIGURE 1. *Combination of wave-induced response measurements and a mathematical model can be used to deduce information about the on-site sea state.* (Nielsen et al., 2016)

64 **2.1. Main Assumption.** In mild and moderate wave climate, the wave-induced six degrees-of-freedom  
65 motion of a ship and associated structural loads are often assumed to be linear with the incident waves,

66 meaning that the amplitudes of those responses are proportional to the wave amplitudes in regular waves.  
 67 Consequently, the responses can be quantified in irregular waves by adding together results from regular  
 68 waves with different amplitudes, wavelengths and propagation directions.

69 The linear assumption between waves and associated responses facilitates the use of transfer functions, or  
 70 response amplitude operators (RAOs), that express how waves are *transferred* into responses. State-of-the-  
 71 art techniques for calculation of RAOs include 3-dimensional panel codes considering potential wave theory;  
 72 sometimes supplemented with CFD based on the full set of Navier-Stoke's equations and/or considering  
 73 other nonlinear effects. Nonetheless, strip theory calculations are still widely used, due to their adequate  
 74 degree of approximation, and often they provide good results.

75 In theory, RAOs are not necessarily accurate in severe waves, where a nonlinear relationship between waves  
 76 and responses would/could occur. In practice, however, many studies have shown that even in severer wave  
 77 conditions, RAOs can be still used to calculate responses of ships.

78 **2.2. Frequency and Time Domain Approaches.** The majority of previous work on the wave buoy analogy  
 79 (e.g. Hua and Palmquist, 1994; Iseki and Ohtsu, 2000; Tannuri et al., 2003; Nielsen, 2006, 2008b; Pascoal  
 80 et al., 2007; Montazeri et al., 2016a) is based on a solution formulated entirely in the frequency domain.  
 81 This is illustrated in Figure 2, where a response spectrum is combined with RAOs, using spectral analysis,  
 82 so that an estimate of the sea state is given in terms of a wave (energy) spectrum. Studies have shown that, in  
 83 practice, wave estimation is improved by (optimally) selecting a set of three simultaneous vessel responses  
 (Nielsen, 2006).

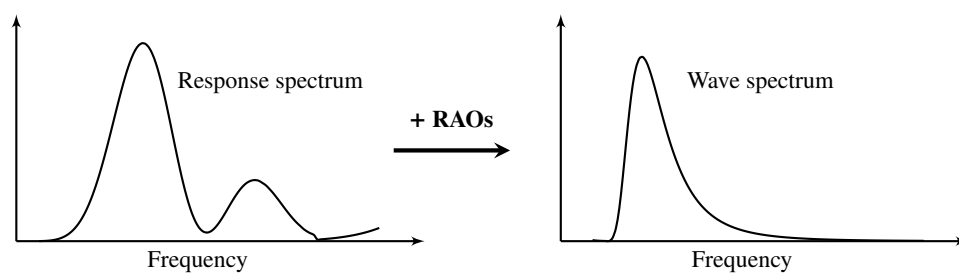


FIGURE 2. Main principle of the wave buoy analogy when it is formulated in the frequency domain. (Nielsen et al., 2016)

84

85 Instead of a solution formulated in the frequency domain, derived by use of spectral analysis and with possible  
 86 disadvantages, it has been suggested by Nielsen et al. (2015, 2016) to make the fitting of the *measured*  
 87 response and the corresponding *theoretically* calculated one directly in the time domain (Fig. 3). In this

88 sense, the approach is similar to a previous work by Pascoal and Soares (2009) that also formulate the gov-  
 89 erning equation directly in the time domain. However, the latter method (Pascoal and Soares, 2009), based  
 90 on Kalman filtering, relies completely on availability of accurate RAOs, which is the main difference to the  
 former works (Nielsen et al., 2015, 2016) as will be outlined in Section 4.

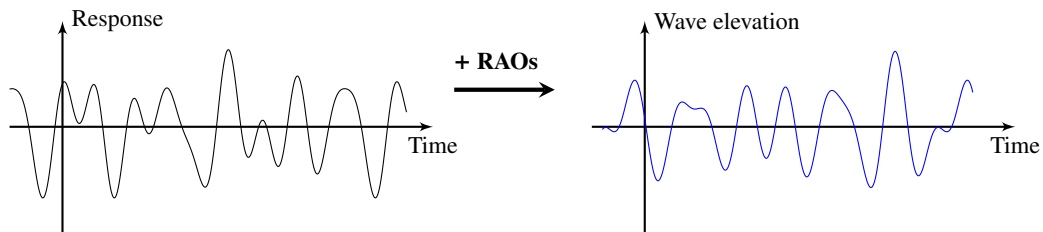


FIGURE 3. *Conceptually, the wave buoy analogy can be formulated directly in the time domain to give the actual wave elevation at the site of the vessel.* (Nielsen et al., 2016)

91

92 In the next two sections, 3 and 4, the fundamentals of the techniques used for, respectively, frequency domain  
 93 and time domain shipboard SSE are briefly described. As such, the sections can be read separately and  
 94 have to some extent been formulated as stand-alone sections, which means that repetitions of fundamental  
 95 assumptions and background occur.

96

### 3. FREQUENCY DOMAIN APPROACHES FOR SSE

97 Shipboard SSE is often considered in the frequency domain. Strictly speaking, the linear assumption about  
 98 waves and associated responses needs, in this case, to be supplemented with additional assumptions: Firstly,  
 99 the ocean waves and associated responses represent ergodic random processes (e.g. Ochi, 1990), so that  
 100 stationarity, in a stochastic sense, applies within a certain period of response records at each estimation  
 101 sequence. Secondly, the speed and the course of the ship (relative to waves) are constant in that period. Thus,  
 102 response measurements from the particular period can be processed by spectral analysis using standard Fast  
 103 Fourier Transformation (FFT) or multivariate autoregressive procedures (Nielsen, 2005, 2006), where the  
 104 latter may sometimes be chosen because of the ability to automatically select the *appropriate* amount of  
 105 smoothing; based on an order selection criterion. Traditionally, the mathematical model of shipboard SSE  
 106 has then been formulated in terms of a comparison between the *measured* and the *theoretically calculated*  
 107 spectral energy distribution of the considered responses.

108 **3.1. Comparison of Spectral Energy Distribution.** A set of ship responses is considered, and the complex-  
 109 valued transfer functions,  $H_i(\omega_e, \chi)$  and  $H_j(\omega_e, \chi)$  for the i-th and j-th responses, yield the theoretical rela-  
 110 tionship between the i-th and the j-th components of the response spectra  $S_{ij}(\omega_e)$  and the directional wave  
 111 spectrum  $E(\omega_e, \chi)$  through the following integral equation

$$S_{ij}(\omega_e) = \int_{-\pi}^{\pi} H_i(\omega_e, \chi) \overline{H_j(\omega_e, \chi)} E(\omega_e, \chi) d\chi \quad (1)$$

112 where  $\omega_e$  and  $\chi$  are the encounter wave frequency and the relative wave heading, respectively, and the bar  
 113 denotes the complex conjugate. The theoretical relationship expressed by Eq. (1) can be directly compared to  
 114 a set of corresponding measured response spectra. Thus, the comparison constitutes the governing equation  
 115 of the estimation problem that can be solved mathematically as a minimisation. It is vital to note that the  
 116 wave spectrum is advantageously estimated in the wave frequency ( $\omega$ ) domain. This means that the speed-  
 117 of-advance - the so-called triple-valued function - problem in following sea needs to be considered. This  
 118 problem, governed by the Doppler Shift, has been properly incorporated by Iseki and Ohtsu (2000), and in  
 119 doing so, the mathematical relation between encountered (wave) frequency and true frequency is secured;

$$\omega_e = \omega - \omega^2 A \quad , \quad A = \frac{U}{g} \cos \chi \quad (2)$$

120 where  $U$  is the forward speed of the ship, and  $g$  is the acceleration of gravity. The *triple-valued function*  
 121 problem exists when  $\omega_e < \frac{1}{4A}$  since, in this case, three wave frequencies correspond to one (positive)  
 122 encounter frequency.

123 It should be understood that the left-hand side of Eq. (1) is estimated by measured data while the right-hand  
 124 side is obtained through theoretical calculations. Consequently, a minimisation problem can be formulated  
 125 and, casting the expressions into matrix notation, the objective is to minimise

$$\chi^2(\mathbf{x}) \equiv \|\mathbf{A}\mathbf{f}(\mathbf{x}) - \mathbf{b}\|^2 \quad (3)$$

126 where  $\|\cdot\|$  represents the  $L_2$  norm. In the equation, the vector function  $\mathbf{f}(\mathbf{x})$  expresses the wave spectrum  
 127  $E(\omega, \chi)$  and the vector  $\mathbf{b}$  contains the elements of the measured response spectra  $S_{ij}(\omega_e)$ , while the coef-  
 128 ficient matrix  $\mathbf{A}$  basically has its elements derived from the complex-valued transfer functions. Details are  
 129 given by Nielsen (2006).

130 The minimisation problem given by Eq. (3) can be handled by different approaches. Two approaches that  
 131 have received particular interest are formed by *Bayesian modelling* and *parametric modelling*. Bayesian  
 132 modelling relies on finding the spectral components of a (discrete) frequency-directional wave spectrum,  
 133 whereas parametric modelling assumes the directional wave spectrum to be formed by a set of parameterised  
 134 wave spectra, e.g., JONSWAP using directional spreading parameters. Reports about the two procedures

135 have been given in many studies (Iseki and Ohtsu, 2000; Iseki and Terada, 2002; Nielsen, 2006, 2008b;  
 136 Pascoal and Soares, 2008; Tannuri et al., 2003; Pascoal et al., 2007; Simos et al., 2007), considering both  
 137 simulated data and full-scale measurements with and without forward speed; and comparisons between the  
 138 two modelling procedures have also been made. However, as pointed out by Nielsen and Stredulinsky  
 139 (2012) and Nielsen et al. (2013), the two approaches should not be seen as competitors but rather as  
 140 complementary, since each procedure has its own advantages and disadvantages.

141 **3.2. Energy Equivalence: Comparison of Spectral Moments.** In a recent PhD study, Montazeri (2016)  
 142 suggests to formulate the governing equation from an energy conservation point-of-view, since the integrated  
 143 variant of Eq. (1) is considered. Thus, the mathematical model is based on an equivalence of the spectral  
 144 moments calculated by integrating the two sides of Eq. (1) with respect to frequency. Again, a *set* of  
 145 responses is considered simultaneously using cross-coupling terms so that the governing equations read

$$\int_{\omega_{e,l}}^{\omega_{e,h}} S_{ij}(\omega_e) d\omega_e = \int_{\omega_l}^{\omega_h} \int_{-\pi}^{\pi} H_i(\omega, \chi) \overline{H_j(\omega, \chi)} E(\omega, \chi) d\chi d\omega \quad (4)$$

146 where indices  $l$  and  $h$  correspond to lower and higher frequency limits, respectively. The actual values  
 147 of these limits are determined through a partitioning technique (Montazeri, 2016) introduced to separately  
 148 estimate wind sea and swell components of the wave system, see Figure 4. The details of this technique are  
 149 given by Montazeri et al. (2016a) and Montazeri (2016), but it is noteworthy that the *ocean wave system*  
 150 is expressed through the sum of two parameterised wave spectra; one for swell and one for wind sea, and  
 151 each taking the form  $S_{wave}(\omega)$  of a general unidirectional spectrum for developing seas (Boukhanovsky and  
 152 Soares, 2009):

$$S_{wave}(\omega) = \alpha g^2 \omega^{-r} \exp(-\beta \omega^{-n}) \gamma^{\exp\left[\frac{-(\frac{\omega}{\omega_p} - 1)^2}{2\sigma^2}\right]} \quad (5)$$

153 where the fitting parameters are  $[\alpha, \beta, \gamma, \sigma, \omega_p, r, n]$ . A directional spectrum is obtained as

$$E(\omega, \theta) = S_{wave}(\omega) D(\theta|\omega) \quad (6)$$

154 with  $D(\dots)$  being a spreading function for wave direction  $\theta$ ; satisfying the normality condition  
 155  $\int_{-\pi}^{\pi} D(\theta|\omega) d\theta = 1$ . In its physical understanding, the equal sign in Eq. (4) should be read like "nearly  
 156 equal to", so that the values of the fitting parameters, including the spreading function, are optimised by  
 157 minimising the difference between the left- and right-hand sides of Eq. (4), with the wave spectrum  $E(\omega, \chi)$   
 158 specified by Eq. (6)\*; leaving all details to Montazeri et al. (2016a) and Montazeri (2016).

159 For the set of governing equations (Eq. 4) it is important to note that the right-hand side is explicitly written  
 160 with account to the true (wave) frequency; and *not* the encounter frequency as is the case of the left-hand side

---

\*Wave direction  $\theta$  will be directly related to relative wave heading  $\chi$  taking ship course into account.



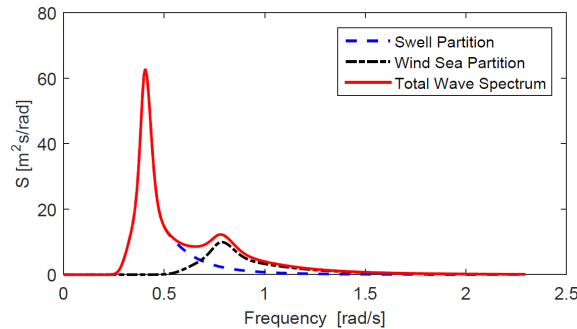


FIGURE 4. *Spectral partitioning of wave spectrum into swell and wind sea components.*  
(Montazeri, 2016)

161 that represents the measurements. This particular formulation, with no need to transform between the two  
 162 frequency domains for the theoretical calculation (i.e., the right-hand side), is possible since the energy must  
 163 be the same in the two domains. Consequently, the exclusive consideration of equations based on energy  
 164 conservation has the (positive) effect that the 1-to-3 relationship between encounter and wave frequency in  
 165 following sea has not to be considered.

166 Compared to the other frequency-domain principle, outlined in subsection 3.1, the ambition with the 'energy-  
 167 equivalence principle', as stated by the authors (Montazeri, Nielsen and Jensen, 2016), is partly to make a  
 168 practical robust procedure and partly to increase the computational efficiency of the wave buoy analogy;  
 169 obviously, not compromising the ability to provide accurate sea state estimates.

170 **3.3. Disadvantages of Frequency Domain Approaches.** The outcome of the wave buoy analogy, when  
 171 formulated in the frequency domain, consists of the on-site wave system's complete energy distribution,  
 172 with frequency and directional information, and thus the approach is applicable to general decision support  
 173 systems for safe and efficient marine operations. As reported in the literature, reasonable estimates of the  
 174 wave spectrum can be expected (Nielsen, 2006, 2008b; Nielsen and Stredulinsky, 2012; Nielsen et al., 2013;  
 175 Montazeri et al., 2016a), but the accuracy of the estimated sea state depends inherently on reliable trans-  
 176 fer functions. Furthermore, the accuracy is highly dependent on the required spectral (response) analysis;  
 177 hence, stationarity, *or* not, of the measurements may potentially influence the outcome (Møgster, 2015; Iseki  
 178 and Nielsen, 2015). In principle, stationary operational conditions are necessary because a minimum time  
 179 window, in the order 10-15 minutes, is needed to perform the spectral analysis. The reason is that if condi-  
 180 tions are not stationary during the considered period, either because of a changing sea state or, more likely,  
 181 as a result of speed and/or heading changes of the vessel, the sea state estimates are likely to be unreliable.  
 182 Moreover, the need for a certain minimum time period has another consequence, as it implies that estimates,

183 strictly speaking, are not real-time but will be backdated; which in turn may negatively influence response  
184 predictions made ahead of measurements, as discussed by Nielsen and Iseki (2015).

185 Altogether, these disadvantages of the frequency domain approaches have initiated studies where the solu-  
186 tion, i.e. sea state estimate, is sought for directly in the time domain; to better accommodate partly non-  
187 stationary conditions. Moreover, work exists, in the time domain, to estimate the peak period of the sea  
188 state, with no other input than the response signal itself (Belleter et al., 2015; Brodtkorb et al., 2015). In  
189 the following, one of the time domain approaches looks at coupling this entirely "signal-based" estimation  
190 concept with the use of RAOs in a *stepwise procedure* to partly mitigate the fact that RAOs are always  
191 imperfect to some degree.

#### 192 4. TIME DOMAIN APPROACHES FOR SSE

193 The central point of the procedures is a formulation of the estimation problem directly in the time domain,  
194 where focus is on real-time sea state updates obtained from continuous response measurements, with no  
195 need to consider a past measurement period.

196 Until now, only few works consider approaches for shipboard SSE directly in the time domain and, so  
197 far, the procedures, like those formulated in the frequency domain, rely on availability of accurate RAOs.  
198 Indeed, this is so for an elaborate procedure, building on a framework established by *Kalman filtering*, which  
199 will be addressed subsequently. However, as will be noted further below, it is possible to make a stepwise  
200 estimation procedure which couples an entirely *signal-based* procedure, estimating the peak wave period,  
201 with a *model-based* procedure, estimating wave height and phase. Herein, the signal-based step has no  
202 need for RAOs, whereas the model-based step makes use of RAOs. In the following, the two conceptually  
203 different approaches, based on, respectively, Kalman filtering and the stepwise procedure, will be concisely  
204 accounted for.

205 **4.1. Wave Estimation Based on Kalman Filtering.** An interesting study has been presented by Pascoal  
206 and Soares (2009) that propose a (high-speed) estimation algorithm established in a framework governed  
207 by Kalman filtering. Herein, the waves in-phase and quadrature components are introduced as the state  
208 variables, which means that (intrinsic) information about the actual wave elevation process is included in the  
209 solution. The mathematical details of the procedure are given by Pascoal and Soares (2009), so the following  
210 contains just a brief summary of the approach.<sup>†</sup>

---

<sup>†</sup>The present author has started recently to also work on this concept.

211 The in-phase and quadrature components of a regular wave from (discrete) direction  $\theta_n$ , at discrete time  
 212  $k$ , constitute a set of state variables  $X_k = [x_1, x_2]^T_n$ . Relying on the electric filter analogy (St.Denis and  
 213 Pierson, 1953), an irregular wave would be the sum of a (large) number of regular waves, implying that  
 214 the associated sea state can be given in terms of an equivalent number of sets of state variables. In normal  
 215 conditions, a sea state will be just very slowly varying and the hypothesis is that the *state* (in a Kalman-  
 216 context) at a next discrete time is as the present, except possibly for some variation due to the state noise  $\xi_k$ .  
 217 Thus, the state equation reads

$$X_{k+1} = X_k + \xi_k \quad (7)$$

218 The state equation is supplemented with a measurement equation and, as the wave estimation is based on  
 219 sensor recordings  $r$  of  $m$  available wave-induced responses, this equation is given by

$$r_{mk} = C_{mk}X_k + \psi_{mk} \quad (8)$$

220 where  $C_{mk}$  is the measurement matrix *transferring* the states into a response (output) that is to be compared  
 221 with a corresponding one available from measurement, while  $\psi_{mk}$  is the measurement noise because of  
 222 a sensor's limited capability. The equation is basically the equivalent of Eq. (1), but formulated in the  
 223 time domain, and Eq. (8) represents, analogously, a linear relationship between a single harmonic wave  
 224 component and an associated response component. As a consequence, the measurement matrix  $C_{mk}$  can  
 225 therefore be composed by the available (complex-valued) transfer functions  $H$ . The specific composition  
 226 of the matrix is realised by expressing the measurement equation in its physical understanding, writing  
 227 the irregular response  $r$  as the sum of  $n_f$  harmonic components, each represented in a total of  $n_\theta$  wave  
 228 directions:

$$r = \text{Re} \left( \sum_{j=1}^{n_f} \sum_{i=1}^{n_\theta} H_{ji} \times (X_{2j-1,i} + \sqrt{-1}X_{2j,i}) \times (\cos(\omega_j t) + \sqrt{-1} \sin(\omega_j t)) \right) \quad (9)$$

229 From the equivalence between Eq. (8) and Eq. (9) it can be seen how the elements of the measurement  
 230 matrix should be assigned. Part of the matrix is shown below for the  $j$ -th frequency,  $i$ -th direction,  $m$ -th  
 231 response and  $k$ -th time instant, respectively

$$C_{jimk} = \begin{bmatrix} \text{Re}[H_{jim}] \cos(\omega_j k \Delta t) - \text{Im}[H_{jim}] \sin(\omega_j k \Delta t) \dots \\ -\text{Im}[H_{jim}] \cos(\omega_j k \Delta t) - \text{Re}[H_{jim}] \sin(\omega_j k \Delta t) \end{bmatrix}^T \quad (10)$$

232 where  $\Delta t$  denotes used sampling time. The full matrix at any point in time  $t_k = k\Delta t$  is built by concatenat-  
 233 ing the submatrices  $C_{jim}$ , leaving  $k$  as the only free index (Pascoal and Soares, 2009).

234 The application of the Kalman filter (e.g. Brown and Hwang, 1992) involves the standard prediction and  
 235 update cycles, and Pascoal and Soares (2009) carefully address many important aspects to consider when

236 implementing the solution scheme in practice; including points about stabilisation of solution, conditioning  
 237 of matrices, tuning of filter gain, etc.

238 It is important to mention that Pascoal and Soares (2009) consider station-kept ships, without forward speed,  
 239 implying that the frequency  $\omega$  in Eq. (9) is the (true) wave frequency. Thus, it is trivial to transform the wave  
 240 spectrum,  $S(\omega_e)$ , estimated in encounter domain to  $S(\omega)$  in the true domain. Although the extension to  
 241 including forward speed is elementary, the practical incorporation is by no means straight-forward because of  
 242 the Doppler shift (Eq. 2), leading to a 1-to-3 relationship between encounter and true frequency in following  
 243 waves when  $\omega_e < \frac{1}{4A}$ , cf. Eq. (2). The basic problem is identical to what is handled by the approach(es)  
 244 formulated in the frequency domain (Section 3). However, it is not possible to use the same type of solution-  
 245 scheme because of the different domains (frequency vs. time). In a new study by Pascoal et al. (2016), the  
 246 effect of forward speed is reportedly included, but the article does not draft an actual implementation of it.  
 247 On the other hand, one possible method to deal with the Doppler shift for ships having forward speed is  
 248 suggested in a recent MSc study by Ding (2016), supervised by the present author. This MSc study shows  
 249 how forward speed can be successfully included, so that the transformation of the wave spectrum from  
 250 encounter to true domain is secured, but the implementation is restricted to long-crested waves. Hence, the  
 251 extension to real ocean waves, i.e. full-scale experimental data, remains. The 'transformation problem' (for  
 252 long-crested waves) is summarised in the following.

253 In case of nonzero forward speed, and for all waves approaching forward of 'beam sea', the transformation  
 254 of the wave spectrum,  $S(\omega_e)$ , in the encounter domain to  $S(\omega)$  in the true (frequency) domain is trivial,  
 255 as Eq. (2) yields a 1-to-1 relationship. For waves approaching behind of 'beam sea' and  $\omega_e < \frac{1}{4A}$ , the  
 256 transformation is non-trivial, since Eq. (2) yields a 1-to-3 relationship; in case of a 1-to-1 relationship  
 257 the transformation is straight-forward and identical to the former situation. If the 1-to-3 relationship oc-  
 258 curs, the (suggested) solution is derived by considering the illustration shown in Figure 5. The *estimated*  
 259 spectral ordinate  $\hat{S}(\omega_e) = A_{e1}$  in encounter-frequency domain is considered. Accordingly, the particular  
 260 ordinate needs to be transferred into three ordinates in the (true) wave-frequency domain;  $\hat{S}(\omega_1) = A_{\omega 1}$ ,  
 261  $\hat{S}(\omega_2) = A_{\omega 2}$ , and  $\hat{S}(\omega_3) = A_{\omega 3}$ , where (only) the frequencies  $\{\omega_1, \omega_2, \omega_3\}$  are known, whereas the values  
 262  $\{A_{\omega 1}, A_{\omega 2}, A_{\omega 3}\}$  are unknown. However, for any parameterised spectrum,  $S^*(\omega|H_s, T_z, \dots)$ , known fre-  
 263 quencies imply known spectral values, if the standard wave parameters ( $H_s, T_z, \dots$ ) are also known. Thus,  
 264 ratios between the spectral ordinates of the parameterised spectrum in the true domain and in the encounter  
 265 domain, respectively, can be formed at the three *known* frequencies:

$$\frac{S^*(\omega_1)}{S_e^*(\omega_e)}, \quad \frac{S^*(\omega_2)}{S_e^*(\omega_e)}, \quad \frac{S^*(\omega_3)}{S_e^*(\omega_e)} \quad (11)$$

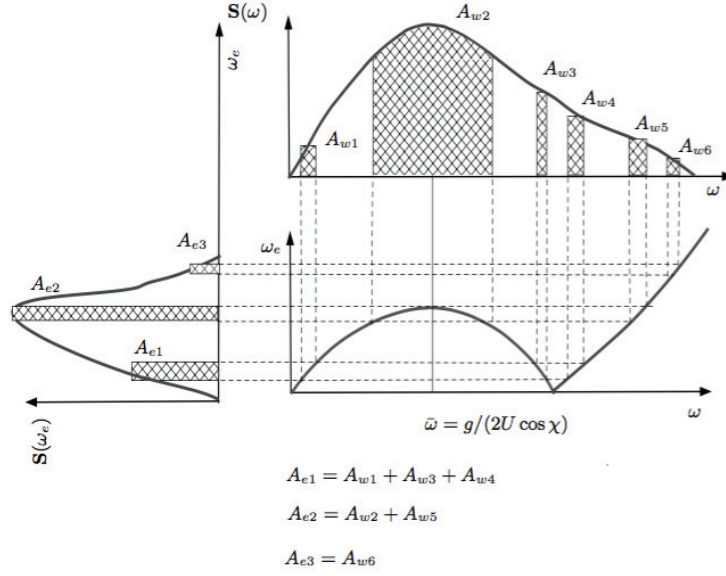


FIGURE 5. Transformation of wave spectrum. (Lewandowski, 2004)

266 taking note that  $S_e^*(\omega_e) = S^*(\omega_1) + S^*(\omega_2) + S^*(\omega_3)$ , cf. Figure 5. It may now be stated, or assumed, that  
 267 the relative distribution of energy in the parameterised spectrum  $S^*(\omega)$  reflects the distribution of the estimat-  
 268 ed "true" spectrum  $\hat{S}(\omega)$ . Hence, ratios similar to Eq. (11) can be formed from the estimated spectrum,  
 269 and, relying on the stated assumption, the following expressions are derived:

$$\frac{\hat{S}(\omega_1)}{\hat{S}(\omega_e)} \doteq \frac{S^*(\omega_1)}{S^*(\omega_1) + S^*(\omega_2) + S^*(\omega_3)} \quad (12)$$

$$\frac{\hat{S}(\omega_2)}{\hat{S}(\omega_e)} \doteq \frac{S^*(\omega_2)}{S^*(\omega_1) + S^*(\omega_2) + S^*(\omega_3)} \quad (13)$$

$$\frac{\hat{S}(\omega_3)}{\hat{S}(\omega_e)} \doteq \frac{S^*(\omega_3)}{S^*(\omega_1) + S^*(\omega_2) + S^*(\omega_3)} \quad (14)$$

270 where the symbol " $\doteq$ " expresses that the ratios are assumed to be identical; not necessarily with a match  
 271 between the pairs of numerators and the pairs of denominators, respectively, on the left- and right-hand  
 272 sides. In Eqs. (12)-(14), the estimated encounter wave spectral ordinate  $\hat{S}(\omega_e)$  is formed by the complex  
 273 wave amplitude, which is the output of the Kalman filtering approach. Thus, the estimated wave spectral  
 274 ordinates  $\hat{S}(\omega_i)$  at the three given wave frequencies  $\omega_i, i = 1, 2, 3$  can be calculated.

275 **4.2. Wave Estimation Based on a Stepwise Procedure.** New conceptual ideas for time-domain-based  
 276 shipboard SSE were addressed recently (Bjerregård, 2014; Nielsen et al., 2015), and one particular method  
 277 has been further studied by Nielsen et al. (2016). Stepwise, the method provides, first, the (characteristic)  
 278 wave period obtained solely from a measured response signal. In the second step, the method combines the

279 use of measurements and corresponding RAOs to estimate wave amplitude and phase (of a regular wave  
 280 train). The partial independency of RAOs is representing a great advantage, as using them in real-world  
 281 applications always is associated with uncertainty due to incomplete knowledge about the input conditions,  
 282 i.e. speed, wave heading, draft, etc.; not to mention (in)accuracies in the calculation of the RAOs themselves.

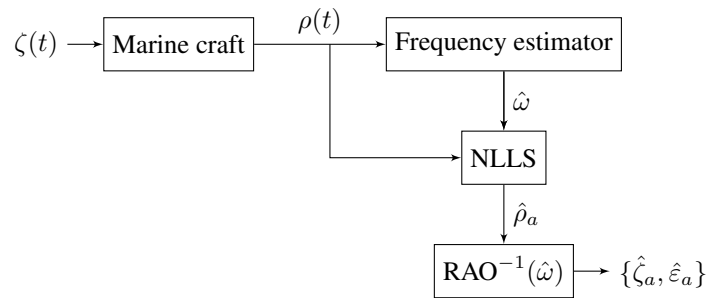


FIGURE 6. *Estimation of wave elevation using nonlinear least squares fitting (NLLS) together with a 'frequency estimator'.* (Nielsen et al., 2016)

283 The details of the stepwise procedure are left to Nielsen et al. (2016), but the principle of the procedure  
 284 is summarised by the block diagram in Fig. 6. The "input" to the marine craft is a wave elevation signal  
 285  $\zeta(t)$  and the "output",  $\rho(t)$ , is a corresponding motion response. From the motion response, the method  
 286 provides, in the first step, the characteristic frequency  $\hat{\omega}$  of the wave signal, and subsequently, in the second  
 287 step, wave amplitude  $\hat{\zeta}_a$  and phase  $\hat{\varepsilon}_a$  are estimated, using a fitted value of the response amplitude  $\hat{\rho}_a$  and  
 288 the inverse,  $\text{RAO}_\rho^{-1}(\hat{\omega})$ , of the corresponding transfer function. The 'Frequency estimator' is based on  
 289 techniques developed within control theory (Aranovskiy et al., 2007; Belleter et al., 2015), whereas the  
 290 estimated response amplitude  $\hat{\rho}_a$  is found from a recursive nonlinear least squares (NLLS) optimisation  
 291 (Nielsen et al., 2016). The estimation process is made on short sequences of data (5-7 wave periods), but  
 292 a new estimation is made on shorter intervals, so that the analysis is based on a "moving window" of  
 293 data recordings, enabling real-time updates/estimates of the wave elevation. However, it is important to  
 294 emphasise that the procedure is still far from mature to be applicable in sea state estimation from full-scale  
 295 measurements data of ships, since the method, so far, is limited to handle only the estimation of regular wave  
 296 trains based on corresponding response measurements from a ship without forward speed.

297

## 5. APPLICATION STUDIES

298 The previous sections have summarised different approaches for shipboard SSE, using the vessel itself as  
 299 a wave buoy. In the past, the author has made numerous studies, alone and with colleagues, applying the  
 300 aforementioned approaches both on simulated response data and on full-scale recordings for estimating the

301 on-site sea state. However, the present section has *not* the aim to widely discuss or show the outcome of  
 302 the studies and analyses; neither by words nor graphically. Instead, the purpose of this section is to point  
 303 out some main findings from the mentioned studies dealing both with the frequency and the time domain  
 304 approaches.

305 **5.1. Frequency Domain SSE.** Two main concepts for sea state estimation in the frequency domain were  
 306 outlined in Section 3; (a) one based on a *direct comparison* of measured and theoretically calculated response  
 307 spectra, and (b) another based on *energy equivalence* focusing on spectral moments. In case of the former  
 308 concept (a), the sea state estimate is obtained by solving for each spectral ordinate of the wave spectrum;  
 309 either by Bayesian modelling, strictly minimising a discrete version of Eq. (1), or by parametric modelling,  
 310 optimising a set of sea state parameters of a given parameterised wave spectrum. In the concept based on  
 311 energy equivalence (b), the sea state estimate is obtained by optimising also for a set of wave parameters,  
 312 but considering the integrated variant of Eq. (1).

313 **5.1.1. Direct Comparison of Spectral Energy Distribution.** As outlined in Subsection 3.1, Bayesian or para-  
 314 metric modelling is applied to produce an estimate of the on-site sea state from comparison between spectra  
 315 of corresponding responses. In either case, the final outcome is a frequency-directional wave spectrum as  
 illustrated in Figure 7.

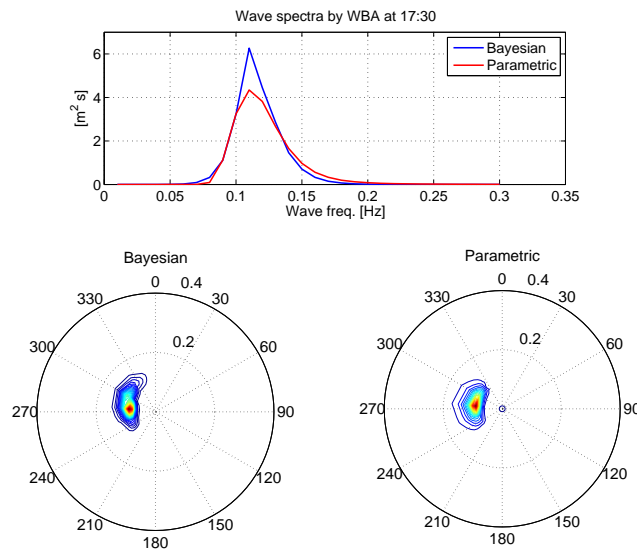


FIGURE 7. Typical wave spectrum obtained by wave buoy analogy; integrated frequency spectrum (top) and directional spectrum (bottom). Nielsen et al. (2013)

317 It is the author's experience that the two techniques - Bayesian and parametric modelling - generally produce  
 318 results with little deviation; in particular when integrated sea state parameters (significant wave height,  
 319 peak period, mean wave direction, etc.) are considered. This has been confirmed in an extensive study by  
 320 Nielsen et al. (2013), where more than 100 hours of response data from an in-service large container ship  
 321 ( $L = 349.0$  m,  $B = 42.8$  m,  $T = 14.5$  m) were analysed. Specifically, it was shown that daily statistics  
 322 of integrated wave parameters agree well between the two sets of results. It is noteworthy that sea state  
 323 estimates by other means, in this case wave radar data and hindcast studies, respectively, produced similar  
 324 results. Figure 7 shows sample plots of the estimated wave spectrum corresponding to one particular instant  
 325 in time (17:30 UTC, 12. Aug. 2011) based on 15 minutes of past measurements data; the results of Bayesian  
 326 ( $H_s = 2.2$  m) and parametric ( $H_s = 2.0$  m) modelling are included. The whole data set, that is, all estimations  
 327 are summarised in Figure 8, where the correlation between results of Bayesian and Parametric modelling,  
 328 including wave radar data, is shown. Results are given for the significant wave height, the zero up-crossing  
 329 period and the relative wave heading (180 deg. is head sea, positive values indicate waves from starboard  
 330 side).

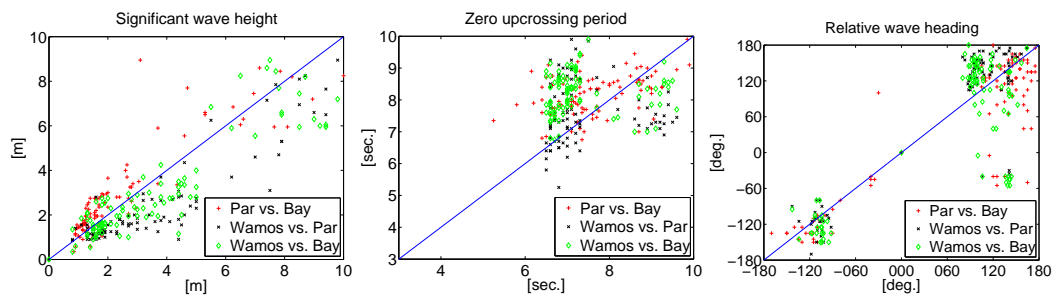


FIGURE 8. *Correlations between estimates of integrated wave parameters as obtained by different shipboard techniques, including parametric (PAR) and Bayesian (Bay) modelling, respectively, and wave radar (Wamos).*

331 In another comprehensive study by Nielsen and Stredulinsky (2012), focus was made on parametric mod-  
 332 elling alone. In this study, sea trials motion data from a small research vessel ( $L = 71.5$  m,  $B = 12.8$  m,  
 333  $T = 4.8$  m) together with data from traditional wave buoys were analysed, and the purpose was to examine  
 334 the sensitivity of sea state estimates by using sets of different vessel responses as input for the wave buoy  
 335 analogy. The trials were carried out in the sea off Nova Scotia, Canada, with the detailed paths shown in  
 336 Figure 9. Sample results are seen in Figure 10, where *estimates* by the wave buoy analogy (parametric  
 337 modelling) are compared with measurements by a Triaxys<sup>TM</sup> buoy. The plots are produced for one spe-  
 338 cific set of responses {roll angle, pitch angle, lateral acceleration} relative to the ship's COG, and it can be  
 339 seen, that in these cases, the agreement is good; even for the multi-modal case shown at the right-hand side.



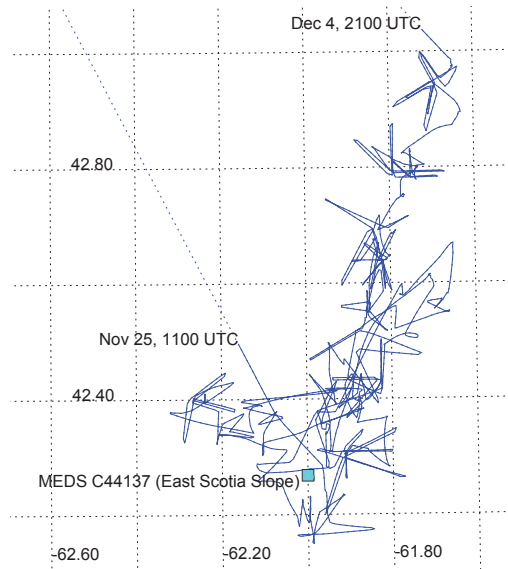


FIGURE 9. Voyage map, including detailed paths of individual trials. (Stredulinsky, 2010)

However, as pointed out in several publications (Tannuri et al., 2003; Pascoal et al., 2007; Simos et al., 2007;

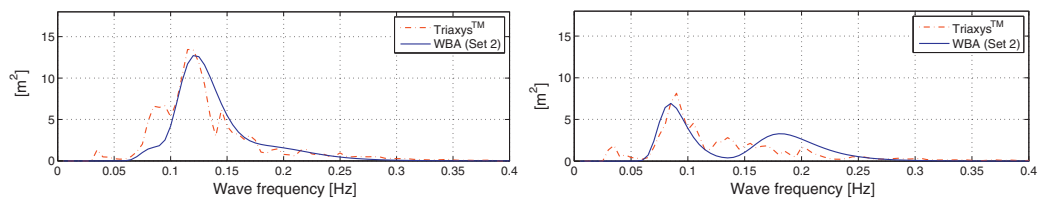


FIGURE 10. Estimated wave spectra (WBA) and 'measured' spectra (Triaxys). (Nielsen and Stredulinsky, 2012)

340

341 Sparano et al., 2008), and thoroughly analysed by Nielsen and Stredulinsky (2012), the selection of different  
 342 combinations of motion components may significantly influence the sea state estimates from the wave buoy  
 343 analogy. It is therefore of a particular concern to make sure that the most sensible set of motions/responses  
 344 always is (automatically) selected. On the other hand, it is by no means straight-forward how to develop  
 345 such a selection process, automatically and in real-time providing the best combination of responses; and  
 346 work in this area is still ongoing with auspicious results in a newly publication by Montazeri et al. (2016b)  
 347 that introduce an approach based on *local sensitivity analysis*.

348 In terms of accuracy and general results in previous studies, it is difficult for the author to favour the one  
 349 modelling procedure to the other, and the computational efficiency of the methods is also comparable. Typ-  
 350 ically, an estimate is provided in about 5 minutes on a standard PC (Intel(R) Core(TM) i7-4600U @ 2.10  
 351 GHz). In practice, this means that "real-time" updates of sea states are possible, as a sea state, for most

352 purposes, is taken to be stationary for periods of approximately 20 minutes; only accounting for the sea state  
353 itself and not any change in vessel speed and/or heading which would lead to nonstationary responses.

354 The most notable difference between the two procedures is probably the ability of the Bayesian method  
355 to (better) estimate wave spectra which do not follow "standard parametric shapes", since each spectral  
356 component of the wave spectrum is solved for (i.e. estimated) individually. On the other hand, for most  
357 practical cases, a *summation* of parameterised wave spectra like, for instance, JONSWAP can be fitted to  
358 represent most ocean wave spectra, like it was seen in Figure 10 for the multi-modal case on the right-hand  
359 side.

360 *5.1.2. Energy Equivalence: Comparison of Spectral Moments.* In the recently developed method, based on  
361 energy equivalence, the ambition by the authors (Montazeri et al., 2016a) was partly to make a practical  
362 robust procedure and partly to increase the computational efficiency of the wave buoy analogy; without  
363 affecting the ability to provide accurate sea state estimates. This ambition is strived for by optimising the  
364 wave parameters of a parameterised spectrum, containing a swell system and a wind sea system, using a  
365 partitioning technique to estimate separately the individual systems. Clearly, due to its recent development,  
366 the method needs to be further tested but, based on preliminary analyses of simulated data, promising results  
367 have been obtained. The performance of the method has been examined thoroughly by Montazeri et al.  
368 (2016a), testing the method's capability to estimate both unimodal and bimodal wave spectra, generated by  
369 pure wind sea and, respectively, mixed sea (wind + swell) conditions. In the study, simulations of motion  
370 responses were carried out for a container ship ( $L = 349.0$  m,  $B = 42.8$  m,  $T = 14.5$  m) similar to that  
371 studied in the previous subsection. Sample results of the study can be seen from Table 1, which presents the  
372 outcome of four test cases, M to P, all representing a mixed sea condition, with a wind sea and a swell part.  
373 From the table, the true wave parameters for both parts appear;  $H_s$  is significant wave height,  $T_p$  is peak  
374 period of the particular spectrum (wind sea or swell),  $\mu$  is relative wave heading,  $s_{max}$  is maximum spreading  
375 parameter (Montazeri et al., 2016a). In the analysis, the true parameters have been used to simulate 15  
376 stochastic wave realisations, including corresponding sets of vessel responses, for each case. Subsequently,  
377 one set of vessel responses at a time has been used as input for the estimation method, and the outcome is  
378 a set of corresponding estimated wave parameters. Thus, mean values and associated standard deviations  
379 were obtained for the 15 realisations of each case (M, N, O, P). It is noteworthy that the sensitivity to the  
380 used set of transfer functions, i.e. RAOs, was investigated by using RAOs calculated by two different sets of  
381 software, say, I and II; but except from that the RAOs have been computed for the same responses under the  
382 exact same input conditions with respect to draft, speed, etc. In the one situation, labelled 'RAO1', the RAOs  
383 of software I were used to both simulate the stochastic wave realisations and to subsequently estimate the sea

TABLE 1. *True and estimated wave parameters obtained in a comprehensive simulation study focusing on SSE based on energy equivalence.* (Montazeri et al., 2016a)

Case		Wind sea				Swell			
		$H_s$ (m)	$T_p$ (s)	$\mu$ (deg.)	$s_{max}$	$H_s$ (m)	$T_p$ (s)	$\mu$ (deg.)	$s_{max}$
I	True	3	8	45	10	5	15	-135	25
	mean (RAO1)	3.1	8.8	66	15	5.2	15	-160	33
	mean (RAO2)	4	8.5	52	15	4.2	15	-101	60
	std (RAO1)	0.7	0.49	10	0	0.6	0.5	12	5.8
	std (RAO2)	0.3	0.55	1.5	5	0.8	0.4	13	20
J	True	3	8	-90	10	5	15	90	25
	mean (RAO1)	3.2	8.6	-106	18	4.4	16.6	98	27
	mean (RAO2)	3.6	9.2	-92	20	3.8	15.1	120	47
	std (RAO1)	0.57	0.75	22	2	1.3	1	7.6	14
	std (RAO2)	0.25	1.3	17	0	0.08	0.6	30	20
K	True	3	8	135	10	5	15	45	25
	mean (RAO1)	2.3	7.3	120	12	5.5	13	49	65
	mean (RAO2)	3.4	6.7	141	15	5.8	12	3	64
	std (RAO1)	0.5	0.8	13	0	0.4	0.1	14	20
	std (RAO2)	0.2	0.2	10	3	0.5	0.1	16	23
L	True	3	8	90	10	5	15	180	25
	mean (RAO1)	3.6	9.1	89	15	5.3	16	174	49
	mean (RAO2)	3.3	6.8	100	18	5.8	14	176	59
	std (RAO1)	0.5	0.1	2	0	0.9	2.7	4	28
	std (RAO2)	1	0.9	2	4	0.8	0.6	11	12

384 state. In the other situation, labelled 'RAO2', RAOs of software I were used for the simulation part, whereas  
385 RAOs of software II were used in the estimation part. This latter situation resembles a situation close(r)  
386 to reality, since the 'input conditions' are never exactly known during full-scale operational service. On  
387 average, the best estimates are observed for 'RAO1'; both in terms of mean values and standard deviations.  
388 However, the important point in this context is that reasonable estimates are found even for 'RAO2'; and the  
389 differences between the results of 'RAO1' and 'RAO2' are barely noticeable from Table 1. Altogether, good  
390 agreement is found between the true and the estimated wave parameters and the study proves both robustness  
391 and computational efficiency of the proposed method. A number of other interesting findings are reported  
392 by the original paper (Montazeri et al., 2016a), but no further remarks are given in the present review.

393 **5.2. Time domain SSE.** The number of studies focusing on the time domain procedures, Kalman filtering  
394 and the stepwise procedure, respectively, are (still) limited compared to the number of frequency-domain  
395 studies. In the future, this is likely to change and the present subsection briefly summarises some of the  
396 existing work that further elaborations may rely on.

397 **5.2.1. Kalman Filtering.** In the first study (Pascoal and Soares, 2009), where Kalman filtering was applied,  
398 the implementation was made for the zero-forward speed case only, and just numerical simulations of motion  
399 data were studied. Similar to any of the frequency domain procedure, the introduction of advance speed in

400 the Kalman filtering approach is elementary, in theory; however, in practice, the implementation is by no  
 401 means straight-forward. The study by Pascoal et al. (2016) addresses partly the effect of forward speed, but  
 402 only in a "qualitative manner", since the work does not describe any details about the actual implementation  
 403 of advance speed. On the other hand, the practical implementation of the advance-speed problem was the  
 404 very topic of a recent MSc thesis by Ding (2016), supervised by the present author. The MSc study shows  
 405 how forward speed can be successfully included, but the implementation is restricted to long-crested waves,  
 406 and, as a consequence, simulation data is studied only for which reason there is still further work to be made.  
 407 One test case from the study is shown in Figure 11, which applies for a container vessel ( $L = 175.0$  m,  
 408  $B = 25.4$  m,  $T = 9.5$  m) at speed 10 knots in stern quartering waves. The plot shows the statistics, i.e.  
 409 average, of totally fifty estimations with the same true input wave parameters:  $H_s = 4.0$  m,  $T_z = 10.0$  s,  
 410  $\chi = 045$  deg. The individual estimation is based on a set of simulations of two responses, heave and pitch,  
 411 realised from a wave elevation process with the given (true) wave parameters. As can be seen from the plot,  
 412 the agreement between the estimated spectrum and the true spectrum is, on average, good; both in terms of  
 413 the total area under the spectra (= energy of the wave system), measured by the significant wave height, and  
 414 the location of the spectra' peak, taken as the peak frequency. However, while the estimated peak frequency  
 415 consistently agrees well with the true peak frequency, some variation in the amount of energy is observed;  
 416 seen from the dashed lines representing the lower and upper extremes of the estimated spectra considering all  
 417 fifty outcomes. Evaluated by numbers, the mean significant wave height is  $\hat{H}_s = 3.7$  m with the coefficient  
 418 of variation being 0.17.

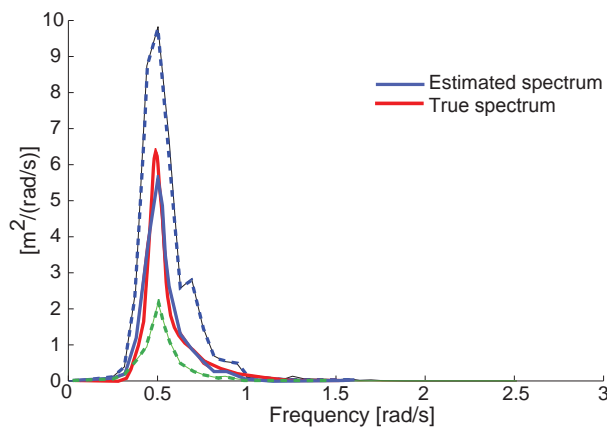
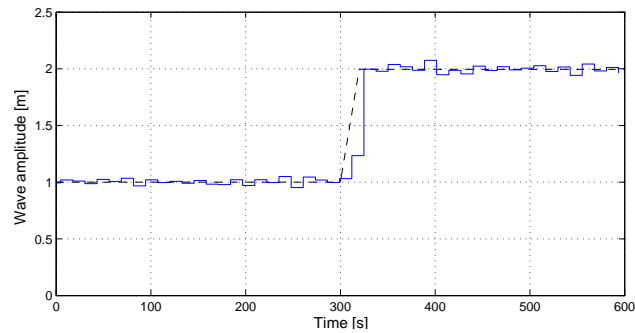


FIGURE 11. Wave estimation using Kalman filtering. Full lines indicate 'average spectrum', while dashed lines represent lowest and highest energy content in estimated spectrum, obtained from fifty sets of estimations. (Ding, 2016)

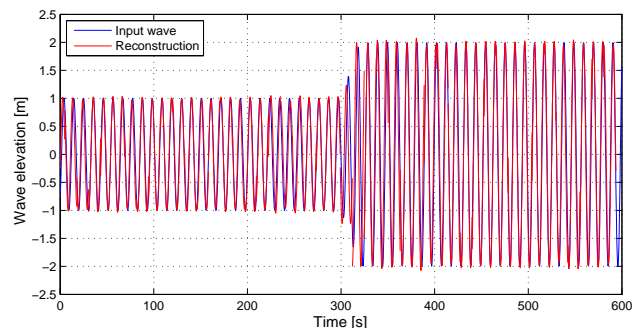
419 *5.2.2. Stepwise Procedure.* The stepwise method is limited to handle only the estimation of regular wave  
420 trains from corresponding response measurements on a ship without forward speed. However, very prom-  
421 ising results have been found in simulation studies and from model-scale experiments outlined by Nielsen  
422 et al. (2015) and Nielsen et al. (2016), respectively. In the former studies, one of the test cases focuses on a  
423 container ship ( $L = 349.0$  m,  $B = 42.8$  m,  $T = 14.5$  m) being exposed to a regular wave train described  
424 by a wave frequency  $\omega = 0.6$  rad/s and an amplitude  $\zeta_a$ . The value of the amplitude is initially 1.0 m but  
425 increases to  $\zeta_a = 2.0$  m during a short period of time [300;320] s. The simulation of the wave train includes  
426 measurement noise, taken as Gaussian white noise produced with a 12 dB SNR and, with this "seaway" as  
427 input, the heave response is simulated in bow-quartering long-crested waves (relative wave heading equal to  
428 135 deg). The wave amplitude estimate, from one simulation, is shown in Figure 12a, where the stairs are  
429 explained because estimation is made on short sequences of data (5-7 wave periods), cf. subsection 4.2. The  
430 complete reconstruction of the wave elevation process can be seen in Figure 12b. The plots show that the  
431 wave parameters, including the actual time history, are estimated with good accuracy. The reason to test on  
432 a case with a somewhat nonphysical sudden change in wave amplitude is merely to evaluate the estimation  
433 method's ability to handle nonstationary data; one of the most important capabilities of the method, since  
434 the method was developed to possess this very property. Indeed, a good result is achieved, and other similar  
435 test cases, but with an abrupt change in wave frequency instead, show equally good behaviour.

436 The stepwise method has also been tested with experimental data (Nielsen et al., 2016), where a 1:30 scale-  
437 model of a platform supply vessel has been exposed to regular waves in the model-basin at the Marine  
438 Cybernetics Laboratory (MCLab) at NTNU, Trondheim, cf. Figure 13.

439 A number of test cases were considered in the experiments and one is presented in Figures 14 and 15. Spe-  
440 cifically, this test case involves wave estimation based on measurements of the heave response in beam sea  
441 condition, see Figure 14, where wave amplitude and period were fixed at {2.0 cm, 1.2 s} and {3.0 cm, 1.7 s},  
442 denoted by Case D and Case E, respectively. In both situations, the actual wave train has been estimated  
443 from 200 seconds data recordings and the results are seen in Figure 15, where the individual plot represents  
444 a zoom of a time window selected arbitrarily from the full estimation sequence lasting 200 seconds in both  
445 cases. In the plots the true amplitude levels are indicated, and it is seen that the estimated results are good.  
446 For the two cases, the estimated (mean) wave periods are  $T_{est} = 1.21$  s and  $T_{est} = 1.71$  s, which agree  
447 nicely with the true periods. In the model-basin, the wave elevation is usually measured by a wave probe  
448 but, unfortunately, the probe was malfunctioning on the days when the experiments were conducted. Con-  
449 sequently, no comparisons can be made between the estimated wave elevation and the actual true one. As  
450 another remark, it should be noted that the "simulations-only" examples, addressed by Nielsen et al. (2015),



(a) Estimated wave amplitude (full line) and true one (dashed line).



(b) Reconstruction of wave elevation process.

FIGURE 12. Sea state estimation based on heave response of a container vessel exposed to bow-quartering regular waves ( $U = 0$  knots), including measurement noise (12 dB SNR).



FIGURE 13. *Experimental facilities at the Marine Cybernetics Laboratory, NTNU.* (Brodtkorb et al., 2015)

451 were studying also the capability to handle nonstationary conditions, such as sudden changes to the (true)  
 452 wave parameters of the wave train to be estimated. The same kind of experiments cannot not be made in the  
 453 model-testing facility, since it is possible only to change the control mechanism of the wave generator after  
 454 a full stop.

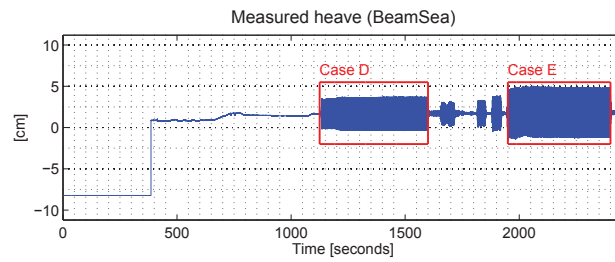


FIGURE 14. *Samples of time history recordings of the response measurements. Cases D and E represents the heave motion. In the post-analysis, the measurements have been averaged to zero-mean.* (Nielsen et al., 2016)

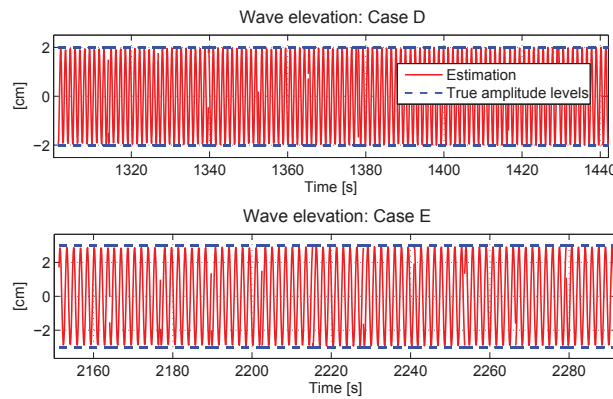


FIGURE 15. *Estimation of wave elevation history from model-scale experiments.* (Nielsen et al., 2016)

455 Obviously, the stepwise estimation method must be extended before it has practical relevance as a means for  
 456 shipboard SSE along with the other techniques addressed in the present paper. Two notable points in future  
 457 suggested studies are: (1) The extension to consider regular wave trains composed by two wave components  
 458 could be beneficial, as it would provide knowledge about how to handle estimation of an irregular wave  
 459 train made up by a (very) large number of regular wave components. Specifically, work could address the  
 460 use of several notch or bandpass filters to select individual harmonic components from a wave spectrum,  
 461 and then use a 'regular wave estimator', like the developed one, for each component. (2) The combina-  
 462 tion/consideration of several responses simultaneously, e.g., {heave; roll; pitch} could (possibly) be used to  
 463 estimate also the relative wave heading.

## 6. CONCLUDING REMARKS

464

465 Procedures for shipboard sea state estimation based on measured vessel responses have been studied and  
466 developed since the 1970'ies. The concept of the wave buoy analogy is still not widely used in practice,  
467 but it is the author's opinion that generally it has matured to a level that would be applicable for shipboard  
468 decision support systems. The concept offers a reasonable alternative to the other shipboard estimating  
469 means, i.e. wave radars, but the concept has lower costs and requires no (or very little) calibration compared  
470 to wave radars. On the other hand, the wave buoy analogy still has weak points which need to be further  
471 addressed. Notably, the ability to handle nonstationary data, which may compromise accuracy/reliability of  
472 real-time sea state estimates. Moreover, it would be beneficial to be able to automatically select the best  
473 combination of available vessel responses; taking into account the effect of different operational conditions.  
474 In the same context, clearly there is a need to introduce fault detection and fault tolerance since, by nature,  
475 all sensor signals will be faulty at times. Obviously, and beyond doubt, this point is of importance to not  
476 only the wave buoy analogy, but to all components of shipboard monitoring and decision support systems. It  
477 is also important to point out, when using a ship as a wave buoy, the inherent limited capability to estimate  
478 waves not necessarily felt by the ship, because of the ship's motion characteristics making it a wave filter.  
479 This issue is touched in a number of previous work (Nielsen, 2006, 2007; Pascoal and Soares, 2008) and a  
480 means to mitigate partly the problem is to use a response such as the relative wave height (Nielsen, 2008a);  
481 based on the instantaneous distance from a fixed point at/on the hull to the sea surface, measured e.g. by  
482 pressure transducers (below the water line) and/or distance meters mounted on the railing. In the same line,  
483 it could be interesting to consider *sensor fusion*, since generally wave radars are considered to yield accurate  
484 estimates of wave period and direction but not always wave height; leaving out any other pro/cons related to  
485 the use of wave radars. In case of sensor fusion, the Kalman filter approach offers a good setting (Pascoal  
486 and Soares, 2009). Finally, efforts should look into associating uncertainty measures on the particular wave  
487 parameter estimates by the wave buoy analogy.

488 The immediate use of sea state estimates onboard a ship is directly coupled to navigational guidance and  
489 decision support to the ship's master and crew, where focus is on safety and fuel consumption. In a somewhat  
490 bigger perspective other uses of shipboard sea state estimations are, for instance, linked to:

- 491 • Ships' operational profiles in a short-term sense and during their lifetime; where an issue is whether  
492 a ship meets the wave scenarios as it was designed for, notably with respect to safety and speed.
- 493 • On-shore performance evaluation of a ship and entire fleets; shipping companies should be able to  
494 make more qualified fuel performance evaluations and comparisons when (reliable) wave data at  
495 actual position(s) is available.



- 496 • Added resistance in waves; related to the previous point, it is desirable to have knowledge about and  
497 to improve models for calculating the added resistance in waves, where experimental data is still  
498 scarce.
- 499 • Global network of 'wave recorders'; the total number of ships navigating the oceans is very large  
500 and, if connected in a network, an enormous amount of wave data/statistics becomes available.
- 501 • Investigation of accidents; a sort of 'black box' could be installed on ships like it is known from the  
502 aviation industry. Thus, with information about responses as well as wave conditions, weather- and  
503 wave-induced accidents would be easier to investigate and analyse.

#### 504 ACKNOWLEDGEMENT

505 The author is pleased to acknowledge his long time collaboration with Professors Jørgen Juncher Jensen,  
506 Technical University of Denmark, and Toshio Iseki, Tokyo University of Marine Science and Technology;  
507 who were the persons to introduce the author to the topic of shipboard sea state estimation. Additionally,  
508 and as a "post-process", the manuscript was improved by the assistance of anonymous reviewers.

#### 509 REFERENCES

- 510 S. V. Aranovskiy, A. A. Bobtsov, A. S. Kremlev, and G. V. Lukyanova. A robust algorithm for identification  
511 of the frequency of a sinusoidal signal. *Journal of Computer and Systems Sciences International*, 46:  
512 371–376, 2007.
- 513 D. J. W. Belleter, R. Galeazzi, and T. I. Fossen. Experimental verification of a global exponential stable  
514 nonlinear wave encounter frequency estimator. *Ocean Engineering*, 97:48–56, 2015.
- 515 M. Bjerregård. Methods for sea state estimation. Master's thesis, Technical University of Denmark, Kgs.  
516 Lyngby, Denmark, June 2014.
- 517 A. V. Boukhanovsky and C. Guedes Soares. Modelling of multip peaked directional wave spectra. *Applied*  
518 *Ocean Research*, 31:132–141, 2009.
- 519 A. H. Brodtkorb, U. D. Nielsen, and A. J. Sørensen. Sea State Estimation Using Model-scale DP Measure-  
520 ments. In *Proc. of MTS/IEEE OCEANS15*, Washington, DC, USA, 2015.
- 521 R. G. Brown and P. Y. C. Hwang. *Introduction to Random Signals and Applied Kalman Filtering*. John  
522 Wiley & Sons, Inc., 3rd edition, 1992.
- 523 F.W. Debord and B. Hennessy. Development of a Generalized Onboard Response Monitoring System.  
524 Technical report, Ship Structure Committee, 1990. Report SSC-349.
- 525 L. Ding. Kalman filtering applied to wave spectrum estimation based on measured vessel responses. Master's  
526 thesis, Technical University of Denmark, Kgs. Lyngby, Denmark, June 2016.

- 527 A. Francescutto. Is It Really Impossible to Design Safe Ships? *Trans. RINA*, 135:163–168, 1993.
- 528 T. Hirayama. Real-time Estimation of Sea Spectra Based on Motions of a Running Ship. *J Kansai Soc Naval*  
529 *Arch*, 204:21–27, 1987.
- 530 J. Hua and M. Palmquist. Wave Estimation through Ship Motion Measurement. Technical report, Naval  
531 Architecture, Department of Vehicle Engineering, Royal Institute of Technology, 1994.
- 532 T. Iseki. Extended Bayesian Estimation of Directional Wave Spectra. In *Proceedings of 23rd Int. Conf. on*  
533 *Offshore Mechanics and Arctic Engineering (OMAE)*, Vancouver, Canada, 2004. ASME.
- 534 T. Iseki and U. D. Nielsen. Study on a Short-term Variability of Ship Responses in Waves. *Journal of Japan*  
535 *Institute of Navigation*, 132:51–57, 2015.
- 536 T. Iseki and K. Ohtsu. Bayesian estimation of directional wave spectra based on ship motions. *Control*  
537 *Engineering Practice*, 8:215–219, 2000.
- 538 T. Iseki and D. Terada. Bayesian Estimation of Directional Wave Spectra for Ship Guidance Systems.  
539 *International Journal of Offshore and Polar Engineering*, 12:25–30, 2002.
- 540 T. Iseki, K. Ohtsu, and M. Fujino. A Study on Estimation of Directional Spectra Based on Ship Motions.  
541 *Journal of Japan Institute of Navigation*, 86:179–188, 1992.
- 542 M. Isobe, K. Kondo, and K. Horikawa. Extension of MLM for Estimating Directional Wave Spectrum. In  
543 *Proceedings of Symposium on Description and Modeling of Directional Seas*, volume A-6, 1984.
- 544 K. Kobune and N. Hashimoto. Estimation of Directional Spectra from the Maximum Entropy Principle. In  
545 *Proceedings of 5th Int. Offshore Mechanics and Arctic Engineering (OMAE) Symposium*, pages 80–85,  
546 Tokyo, Japan, 1986. ASME.
- 547 E. M. Lewandowski. *The Dynamics of Marine Craft: Maneuvering and Seakeeping*. World Scientific, 2004.
- 548 K. Lindemann and N. Nordenstrøm. A System for Ship Handling in Rough Weather. In *Proc. of Fourth Ship*  
549 *Control System Symposium*, volume 7, pages 45–68, Royal Netherlands Naval College, 1975.
- 550 K. Lindemann, J. Odland, and J. Strengehagen. On the Application of Hull Surveillance Systems for In-  
551 creased Safety and Improved Structural Utilization in Rough Weather. *Trans. of SNAME*, 85:131–166,  
552 1977.
- 553 K. Maeda, T. Akashi, and K. Saito. An estimation of ocean wave characteristics based on measured ship  
554 motions (4th report): Directional wave spectrum estimated from full-scale measurements. *J. of the Society*  
555 *of Naval Architects of Japan*, 190:241–246, 2001.
- 556 C. Møgster. Bayesian methods for estimating non-stationary ship response spectra. Master’s thesis, Norwe-  
557 gian University of Science and Technology, Trondheim, Norway, May 2015.
- 558 N. Montazeri. *Estimation of waves and ship responses using onboard measurements*. PhD thesis, Section of  
559 Fluid Mechanics, Coastal and Maritime Engineering, Department of Mechanical Engineering, Technical

- 560 University of Denmark, June 2016.
- 561 N. Montazeri, U. D. Nielsen, and J. J. Jensen. Estimation of wind sea and swell using shipboard measure-  
562 ments - A refined parametric modelling approach. *Applied Ocean Research*, 54:73–86, 2016a.
- 563 N. Montazeri, U. D. Nielsen, and J. J. Jensen. Selection of the optimum combination of responses for Wave  
564 Buoy Analogy - An approach based on local sensitivity analysis. In *Proc. of 13th PRADS*, Copenhagen,  
565 Denmark, 2016b.
- 566 U. D. Nielsen. *Estimation of Directional Wave Spectra from Measured Ship Responses*. PhD thesis, Sec-  
567 tion of Coastal, Maritime and Structural Engineering, Department of Mechanical Engineering, Technical  
568 University of Denmark, May 2005.
- 569 U. D. Nielsen. Estimations of on-site directional wave spectra from measured ship responses. *Marine*  
570 *Structures*, 19:33–69, 2006.
- 571 U. D. Nielsen. Response-based estimation of sea state parameters - influence of filtering. *Ocean Engineering*,  
572 34:1797–1810, 2007.
- 573 U. D. Nielsen. The wave buoy analogy - estimating high-frequency wave excitations. *Applied Ocean*  
574 *Research*, 30:100–106, 2008a.
- 575 U. D. Nielsen. Introducing two hyperparameters in Bayesian estimation of wave spectra. *Probabilistic*  
576 *Engineering Mechanics*, 23:84–94, 2008b.
- 577 U. D. Nielsen and T. Iseki. A Study on Parametric Wave Estimation Based on Measured Ship Motions.  
578 *Journal of Japan Institute of Navigation*, 126, 2012.
- 579 U. D. Nielsen and T. Iseki. Prediction of First-Order Vessel Responses with Applications to Decision Support  
580 Systems. In *Proc. of 5th World Maritime Technology Conference*, Providence, RI, USA, 2015.
- 581 U. D. Nielsen and D. C. Stredulinsky. Sea state estimation from an advancing ship - A comparative study  
582 using sea trial data. *Applied Ocean Research*, 34:33–44, 2012.
- 583 U. D. Nielsen, I. M. V. Andersen, and J. Koning. Comparisons of Means for Estimating Sea States from an  
584 Advancing Large Container Ship. In *Proc. of 12th PRADS*, Changwon, South Korea, 2013.
- 585 U. D. Nielsen, M. Bjerregård, R. Galeazzi, and T. I. Fossen. New Concepts of Shipboard Sea State Estima-  
586 tion. In *Proc. of MTS/IEEE OCEANS15*, Washington, DC, USA, 2015.
- 587 U. D. Nielsen, R. Galeazzi, and A. H. Brodtkorb. Evaluation of Shipboard Wave Estimation Techniques  
588 Through Model-scale Experiments. In *Proc. of MTS/IEEE OCEANS16*, Shanghai, China, 2016.
- 589 M. K. Ochi. *Applied probability and stochastic processes in engineering and physical sciences*. Wiley, 1990.
- 590 R. Pascoal and C. Guedes Soares. Non-parametric wave spectral estimation using vessel motions. *Applied*  
591 *Ocean Research*, 30:46–53, 2008.

- 592 R. Pascoal and C. Guedes Soares. Kalman filtering of vessel motions for ocean wave directional spectrum  
593 estimation. *Ocean Engineering*, 36:477–488, 2009.
- 594 R. Pascoal, L. P. Perera, and C. Guedes Soares. Estimation of Directional Sea Spectra from Ship Motions in  
595 Sea Trials. *To appear in Ocean Engineering*, 2016.
- 596 R. Pascoal, C. Guedes Soares, and A. J. Sørensen. Ocean Wave Spectral Estimation Using Vessel Wave  
597 Frequency Motions. *Journal of Offshore Mechanics and Arctic Engineering*, 129:90–96, 2007.
- 598 J.A. Pinkster. Wave-feed-forward as a means to improve dynamic positioning. In *Proceedings of Offshore*  
599 *Technology Conference (OTC)*, Houston, USA, 1978.
- 600 D.W. Robinson. Voyage Data Recorders - Operating with Safety and Efficiency. In *Proceedings of IMAS90:*  
601 *Marine Technology and the Environment*, London, Institute of Marine Engineers, May 1990.
- 602 K. Saito, K. Maeda, A. Matsuda, and K. Suzuki. An Estimation of Wave Characteristics Based on Measured  
603 Ship Motions (3rd Report). *J. of the Society of Naval Architects of Japan*, 187:77–83, 2000.
- 604 A. N. Simos, J. V. Sparano, E. A. Tannuri, and V. L. F. Matos. Directional Wave Spectrum Estimation  
605 Based on a Vessel 1st Order Motions: Field Results. In *Proc. of 17th International Offshore and Polar*  
606 *Engineering Conference*, Lisbon, Portugal, 2007.
- 607 J. V. Sparano, E. A. Tannuri, A. N. Simos, and V. L. F. Matos. On the Estimation of Directional Wave  
608 Spectrum Based on Stationary vessels 1st Order Motions: A New Set of Experimental Results. In *Proc.*  
609 *of OMAE'08*, Lisbon, Portugal, 2008.
- 610 M. St.Denis and W.J. Pierson. On the Motion of Ships in Confused Seas. *Trans. of SNAME*, 61:280–332,  
611 1953.
- 612 D. C. Stredulinsky. Quest Q319 Sea Trial Summary and Wave Fusion Analysis. Technical Report TM 2010-  
613 051, Defence Research and Development (DRDC) Canada - Atlantic, Dartmouth, NS, Canada, 2010.
- 614 K. Takekuma and T. Takahashi. On the Evaluation of Sea Spectra based on the Measured Ship Motions.  
615 *Trans. of the West-Japan Society of Naval Architects*, 45:51–57, 1973.
- 616 E. A. Tannuri, J. V. Sparano, A. N. Simos, and J. J. Da Cruz. Estimating directional wave spectrum based  
617 on stationary ship motion measurements. *Applied Ocean Research*, 25:243–261, 2003.
- 618 O.J. Waals, A.B. Aalbers, and J.A. Pinkster. Maximum Likelihood Method as a Means to Estimate The  
619 Directional Wave Spectrum and The Mean Wave Drift Force on a Dynamically Positioned Vessel. In  
620 *Proceedings of OMAE2002*, Oslo, Norway, 2002. ASME.